ELSEVIER

International Journal of Pharmaceutics 162 (1998) 77–86

international journal of pharmaceutics

Pegylated liposomal doxorubicin (DOXIL®, CAELYX®) distribution in tumour models observed with confocal laser scanning microscopy

Paul S. Uster [a,*], Peter K. Working [a], Jan Vaage [b]

[a] *SEQUUS™ Pharmaceuticals, 960 Hamilton Court, Menlo Park, CA 94025, USA*
[b] *Department of Molecular Immunology, Roswell Park Cancer Institute, Elm and Carlton Streets, Buffalo NY 14263, USA*

Accepted 7 November 1997

Abstract

The activity of doxorubicin hydrochloride in preclinical tumor models is markedly improved by encapsulation in pegylated liposomes (DOXIL, CAELYX). To understand this response in better detail, spatial and temporal drug distribution in frozen tumor sections was observed with confocal laser scanning (CLS) microscopy. Tumor tissue absorption and distribution phases were markedly altered by pegylated liposome encapsulation. The resultant tumor tissue area under the curve was increased at least several fold over an equivalent dose of free drug. The majority of visible fluorescence was in the nuclear compartment; encapsulated drug apparently leaves liposomes in the interstitial spaces within minutes and appears in the nucleus. Pilot experiments suggest that drug and lipid uncouple at an extracellular location. The increased nuclear exposure to drug is likely responsible for the enhanced therapeutic effect of encapsulation in pegylated liposomes.

1. Introduction

The relative distribution of STEALTH® liposomes between the plasma compartment, macrophage-rich reticuloendothelial organs such as liver and spleen, tumours and other tissues with increased vascular permeability has been described in some detail by several laboratories (Allen and Chonn, 1987; Gabizon et al., 1989; Blume and Cevc, 1990; Klibanov et al., 1990; Allen et al., 1991; Gabizon, 1992). The location and concentration of both the liposome and its drug payload becomes of paramount interest in furthering our understanding of the mechanism of action. Confocal laser scanning (CLS) microscopy is a research tool well suited for studying the spatial and temporal distribution of fluorescent compounds such as doxorubicin hydrochloride in cultured cells in vitro (Kawai et al., 1997) and in vivo

* Corresponding author. Tel.: +1 415 31239011; fax: +1 415 6173080; e-mail: paulu@sequus.com

0378-5173/98/$19.00
PII S0378-5173(97)00415-8

(Vaage et al., 1994; Unezaki et al., 1996). CLS can probe the temporal and spatial biodistribution of fluorescent drug compounds within a given tissue, providing levels of information not available from a chemical analysis of homogenized tissue. The ruby red fluorescence of anthracyclines lend themselves well to visualization in tissue slices and by using microscopy, fixed frozen sections can be used (Forrsen et al., 1996).

In this chapter we shall compare and contrast the tumour distribution of doxorubicin hydrochloride administered i.v. as the drug in solution and encapsulated in the pegylated liposomal delivery system (CAELYX®, also known as DOXIL® in the USA). We briefly review the antitumour activity of both formulations, the methodology developed to study it in vivo and the time course and location in several tumours. We discuss some of our recent findings concerning the location of liposome and drug payload separation. Finally, the chapter concludes with our working model of CAELYX distribution and elimination within tumours.

1.1. Antitumour activity

CAELYX has been found to have therapeutic advantages over unencapsulated doxorubicin hydrochloride in many implanted animal tumour models (Senior, 1988; Papahadjopoulos et al., 1991; Vaage et al., 1993a,b; 1994; Allen et al., 1995; Siegal et al., 1995; Vaage et al., 1995; Zhu et al., 1996; Vaage et al., 1997) and spontaneously-arising canine tumours (Vail et al., 1997). The clinical activity of CAELYX is under investigation as an active agent in Kaposi's sarcoma (Harrison et al., 1995) and various solid tumours (Uziely et al., 1995; Muggia et al., 1997).

AsPC-1, one such example, is a human pancreatic adenocarcinoma xenografted into immunodeficient nude mice The tumour was passaged in animals and for experimental studies removed and dissected into 1 mm^3 pieces. Each piece was then implanted s.c. into the posterior flanks of new mice. Multiple doses of doxorubicin hydrochloride or CAELYX were given by tail vein injection for 5 consecutive weeks starting the day after tumour implantation (arrows, Fig. 1). After a similar cumulative dose of 15 mg/kg, both the doxorubicin hydrochloride and the CAELYX treatment have reduced the tumour burden, but CAELYX is significantly more active in reducing the carcinoma growth rate.

The mechanisms accounting for the improved efficacy of pegylated liposomal doxorubicin hydrochloride are not well understood. How then might the time-course, tissue drug concentration and intra-tumour drug location of CAELYX contribute to an understanding of the increased activity?

2. Materials and methods

The treatment protocols were modified to do CLS microscopy. A single dose of either doxorubicin hydrochloride or CAELYX was given. Multiple doses resulted in necrosis and disintegration of tumour structure in the sections which created interpretation problems. Hence, the sections appear to be rather unremarkable in cytology. Another key difference from efficacy studies is that the tumours were allowed to grow to a larger tumour size in order to facilitate the production of numerous cryostat sections with distinguishing histological landmarks. After the tumours were

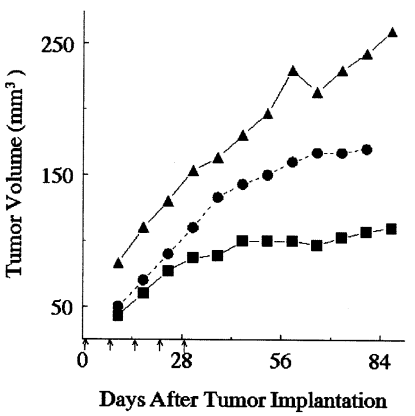

Fig. 1. Relative antitumour effects of doxorubicin hydrochloride (●) and pegylated liposomal doxorubicin (CAELYX, ■) as compared to saline treatment (▲). AsPC-1 human pancreatic adenocarcinoma was implanted s.c. Drug treated animals were given five 3 mg/kg doses 1 week apart. (Adapted from (Vaage et al. 1997))

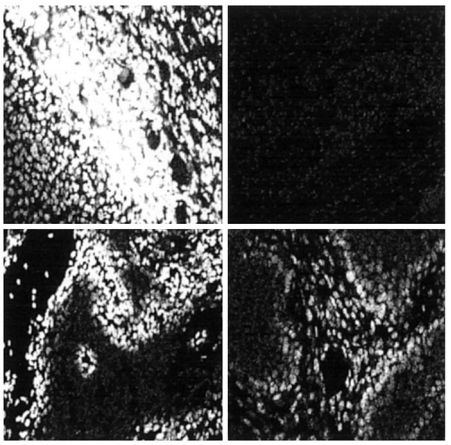

Fig. 2. Drug fluorescence in i.v. treated AsPC-1 pancreatic tumours. Upper row, doxorubicin hydrochloride; lower row, CAELYX. Left column, 2 h post injection; right column; 24 h post injection.

excised they were immediately frozen in liquid nitrogen and stored until cut into 15 μm thick frozen sections with a cryotome. Frozen sections were put on ice cold slides and immersed for 3 min in ice cold Carnoy's solution, followed by quick rinses with ice cold phosphate buffered saline. The slide was then immediately studied for drug fluorescence and the images were recorded as digitized bitmaps for later analysis. After the fluorescence distribution had been recorded, the slide was stained with hematoxylin and eosin and the same fields recorded by video imaging of transmitted light microscopy.

2.1. CLS microscopy of drug distribution in a xenografted pancreatic carcinoma

Fig. 2 illustrates the drug distribution in treated AsPC-1 pancreatic tumours. The hosts of the tumours in the upper row were given free doxorubicin and the lower row had CAELYX administered. The left column is at 2 h post injection and the right column is 24 h post injection. There is a very striking difference in drug fluorescence intensity and its location within the tumour sections. Doxorubicin hydrochloride fluorescence is clearly visible and widespread at 2 h but visually undetectable at 24 h. In contrast, CAELYX fluorescence is noticeable at 2 h, but appears to be restricted to cells near blood vessels. By 24 h CAELYX drug concentration has increased in intensity within the tumour and drug fluorescence has spread throughout the field. It will be noted from this figure that there are differences in both the spatial and temporal intra-tumour distribution. Forrsen et al. have noted analagous contrasts in the spatial distribution of free and liposomal-encapsulated daunorubicin (Forrsen et al., 1996). However, the elimination phase of free daunorubicin in their study is reported to be markedly slower than our observations on free doxorubicin.

In this experiment the fluorescence intensity of several fields was quantified by attaching a photomultipler to the camera eyepiece and measuring the total intensity (Fig. 3). Doxorubicin hydrochloride concentration in the tumour is definitely greater immediately after injection, but declines quickly. The absorption and elimination phases of CAELYX in the tumour were considerably longer. Drug fluorescence peaked within 24–48 h and persisted for at least 6–7 days. Although CAELYX never reached the initial fluorescence

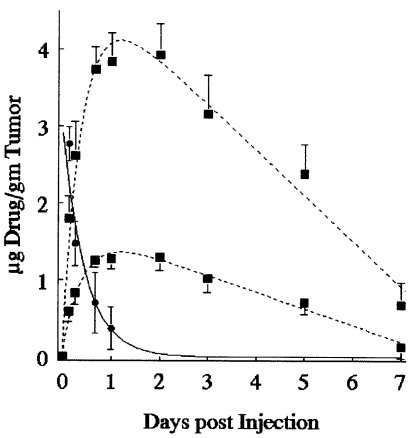

Fig. 3. Micro-fluorimetric analysis of doxorubicin hydrochloride (●) and doxorubicin encapsulated in polyethylene-glycol coated liposomes (CAELYX) in subcutaneous implants of AsPC-1. The high–low spread in values for CAELYX (■) reflects the potential range of fluorescence auto-quenching assuming that all the drug is released (low limit) or that all of the doxorubicin was encapsulated (high limit). Each mouse received a 3.0 mg/kg drug dose i.v. (adapted from (Vaage et al. 1997)).

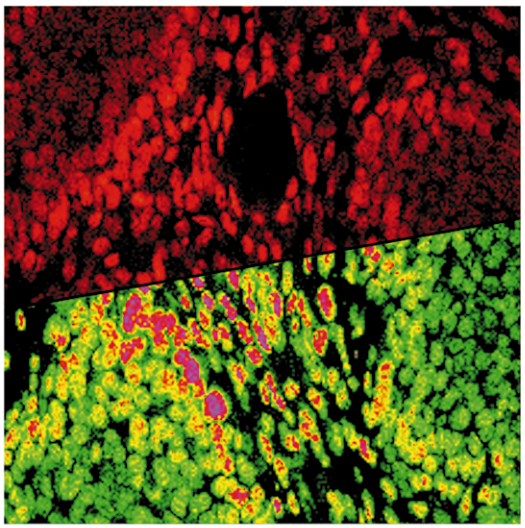

Fig. 4

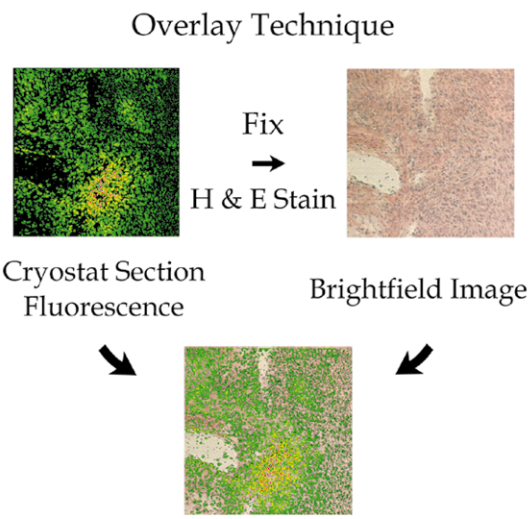

Fig. 5

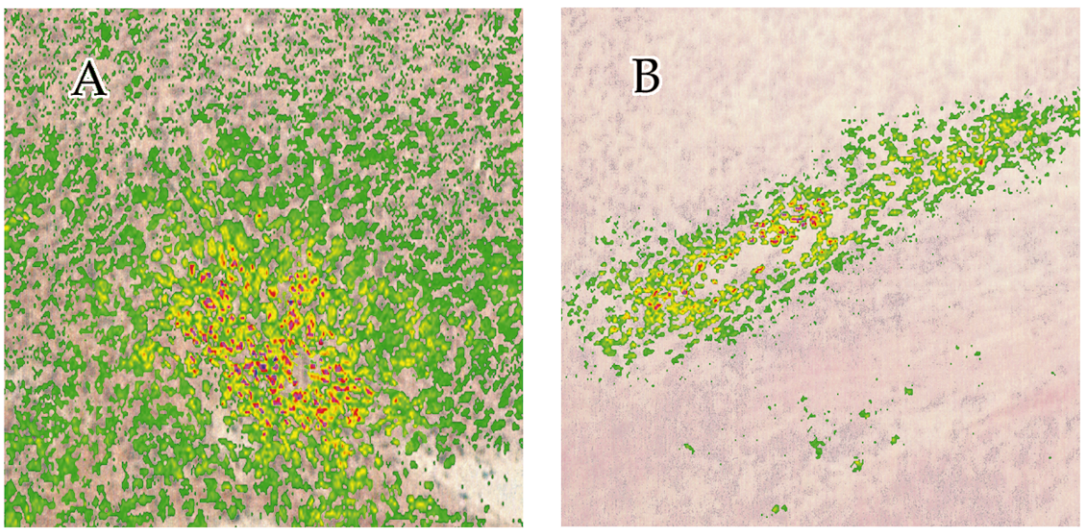

Fig. 6

Fig. 4. Conversion scheme from fluorescence intensity to color spectrum.
Fig. 5. Computer assisted overlay of fluorescence distribution and histological landmarks.
Fig. 6. PC-3 pancreatic carcinomas were implanted s.c. in nude mice and allowed to establish for 5 weeks. The panels follow a single 6 mg/kg dose of doxorubicin hydrochloride or CAELYX given intravenously at time zero. Panel A, doxorubicin hydrochloride at 1 h post-dose; Panel B, CAELYX distribution at 1 h.

intensity of the free drug, fitting the data to a bi-exponential equation indicates that the tissue area under the curve (AUC) of CAELYX is at least six times greater than doxorubicin hydrochloride.

The information content of such images can be enhanced by converting drug fluorescence intensity into a computer generated spectrum (Fig. 4). The vertical bars in the middle are scales representing intensities ranging from 1 to 256 and

ranging from black background to saturated monochromatic fluorescence. In the right bar background black increases in green intensity until saturation is reached. Then the wavelengths move through the spectrum with increasing greater tissue drug concentration. This brings out quite a bit more of the drug distribution. It can now be detected visually in locations where it is too dim to be directly observed without saturating the top end of the intensity scale.

We also devised a graphical strategy for superimposing the fluorescence and transmitted light images (Fig. 5). Drug fluorescence in the frozen section is first recorded and the section is then fixed, stained and re-examined to photograph the same field in transmitted light. The black background pixels of the fluorescence are removed. The resulting digital transparency is layered over the stained image of the same field. Using anatomic landmarks, both images are aligned to superimpose drug distribution upon the field.

2.2. CLS microscopy of drug distribution in a xenografted pancreatic carcinoma

The PC-3 prostatic carcinoma is another xenografted human tumour in which CAELYX shows improved activity over doxorubicin hydrochloride. These tumours have been allowed to establish for 5 weeks in the nude mouse host and then given a single i.v. dose of 6 mg/kg doxorubicin hydrochloride or CAELYX. In this series of figures, we look over a low field magnification at selected tumour sections.

There is a marked difference in the drug distribution 1 h after injection of the drug dose (Fig. 6A, B). Doxorubicin hydrochloride has a much more broadly spread distribution. There is an intense drug concentration around several blood vessels and stromal tissue. Relatively low (green) drug intensities are distributed over much of the broad field of view. In contrast, CAELYX distribution is highly localized around the blood vessels. As the section seems to be cutting through a vessel at an oblique angle, all of the green distribution observed may be perivascular. Although there are some hotspots of yellow and red adjacent to the vessel. there is less of these elevated drug concentrations as in the doxorubicin hydrochloride-treated section.

At 6 h post intravenous injection the distribution of both has definitely changed (Fig. 7). With respect to doxorubicin hydrochloride, the broad initial front of the drug may be retreating because of re-distribution and metabolism to non-fluorescent products. The greatest drug concentrations remain near blood vessels. On the other hand, CAELYX appears to have increased its distribution into the tumour. Numerous hot spots are visible along the highly vascularized margin of this tumour section (Fig. 7B).

Just 24 h after dosing doxorubicin hydrochloride has all but disappeared. leaving remnants of fluorescence activity (Fig. 8A). CAELYX activity, in contrast, is even more substantial and by now appears to have spread some distance from the blood vessels (Fig. 8B).

At 72 h post CAELYX injection, there is still considerable drug fluorescence in CAELYX treated tumours (Fig. 9) while drug fluorescence has not been detectable in doxorubicin hydrochloride treated tumours for more than 24 h. At this time point the margin of CAELYX drug fluorescence gives the impression of starting to recede. However, even at 5 days there is a considerable amount of the drug remaining in the tumour section and it is discernible at 1 week post-injection (Fig. 10).

The drug concentration in the previous sections was quantified from the digitized fluorescence image using scanning software. The program was asked to select the tumour area and then to calculate the average fluorescence intensity per unit area. Again, our qualitative visual observations are congruent with the fluorescence intensities (Fig. 11). The graph does not, of course, illustrate the spatial contrasts. Doxorubicin hydrochloride concentration is greatest at the earliest time point, then fluorescence intensity drops quickly. CAELYX drug fluorescence peaks at 24 h and persists for at least 7 days. Best fit of the data to an exponential model indicates the tissue AUC after CAELYX administration is 14 times greater than that of doxorubicin hydrochloride in this particular model.

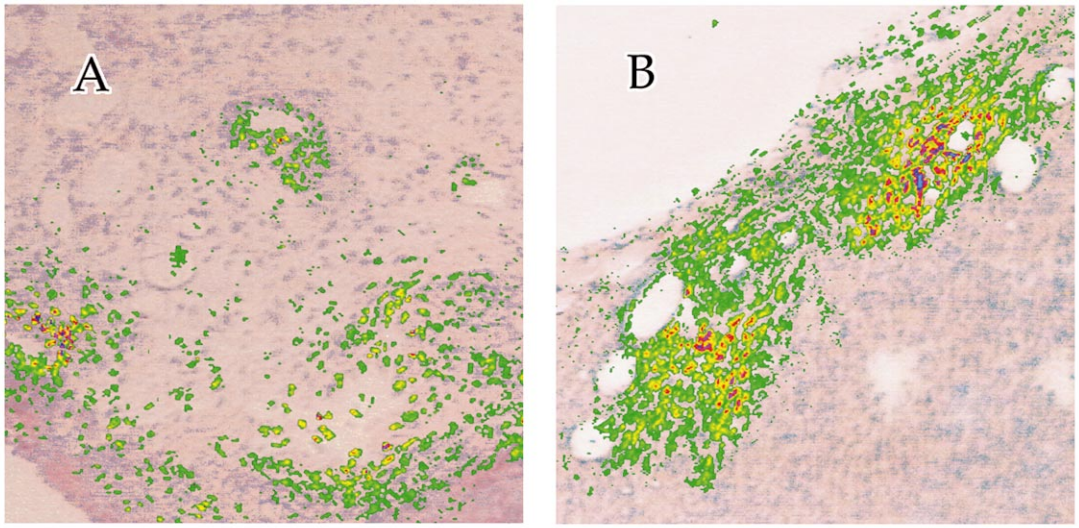

Fig. 7

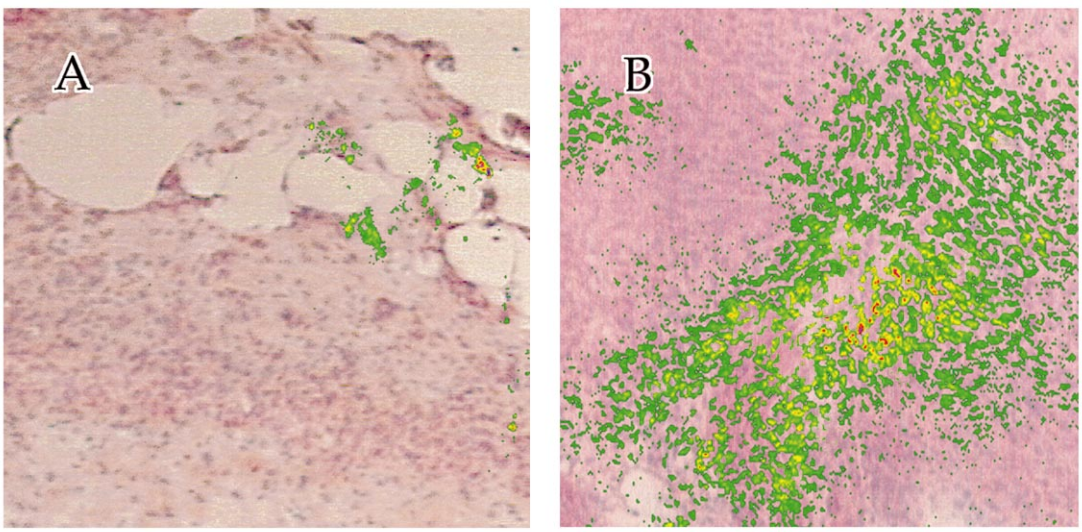

Fig. 8

Fig. 7. PC-3 pancreatic carcinoma 6 h after 6 mg/kg dose of: Panel A, doxorubicin hydrochloride; Panel B, CAELYX.
Fig. 8. PC-3 pancreatic carcinoma 24 h after 6 mg/kg dose of: Panel A, doxorubicin hydrochloride; Panel B, CAELYX.

2.3. CLS microscopy of intracellular drug location in a syngeneic mammary carcinoma

The time course and spatial distribution of doxorubicin hydrochloride and CAELYX in the MC-2 mouse mammary carcinoma are similar to the xenografts. Observations at higher magnification in all three tumour models made it clear that the drug fluorescence is not uniformly distributed within cells. Fig. 12A, B are representative sections taken from MC-2 mammary carcinomas removed only 1 min after drug treatment. The same short-time distribution as seen in the two xenograft models is evident here as well. Doxorubicin hydrochloride is evenly distributed everywhere throughout the field of view, and CAELYX

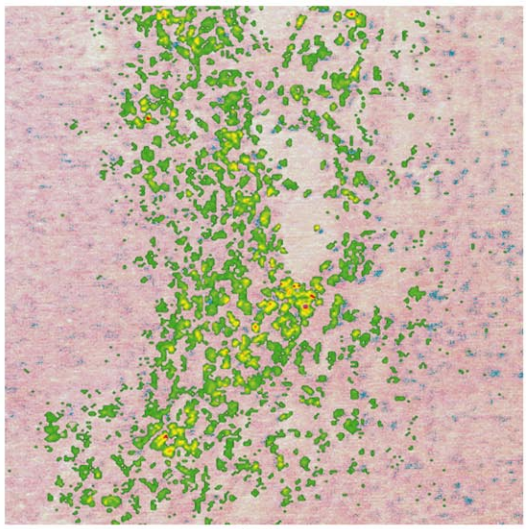

Fig. 9

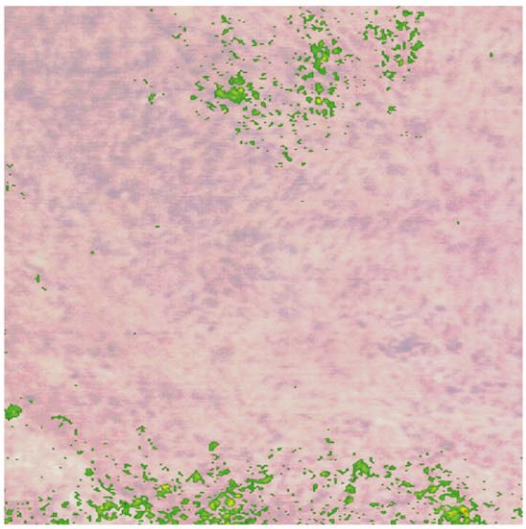

Fig. 10

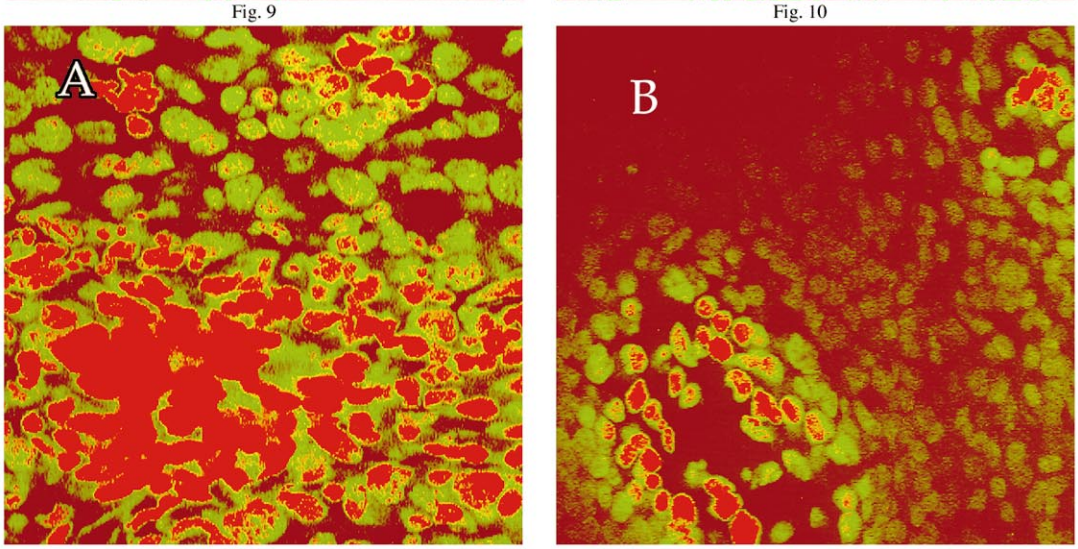

Fig. 12

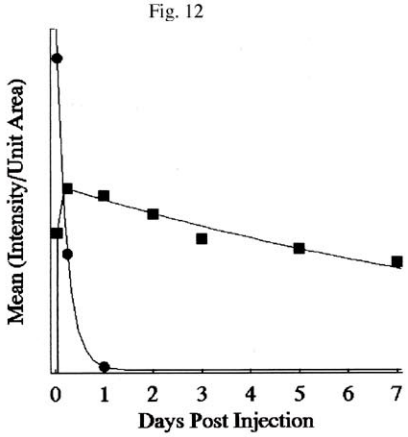

Fig. 11

Fig. 9. PC-3 pancreatic carcinoma 96 h after 6 mg/kg dose of CAELYX.
Fig. 10. PC-3 pancreatic carcinoma 168 h after 6 mg/kg dose of CAELYX.
Fig. 11. Digitized analysis of PC-3 sections treated with doxorubicin hydrochloride (●) or CAELYX (■). The fluorescence intensity/unit area values assumes all drug is released from the liposomes.
Fig. 12. Fluorescence distribution 1 min after doxorubicin hydrochloride (A) or CAELYX) administration. MC-2 mammary carcinomas are implanted s.c. in C3H mice and allowed to grow for 2 weeks, during which time a single dose of 10 mg/kg doxorubicin hydrochloride or CAELYX is given i.v.

distribution is largely restricted to the immediate area around the blood vessel. However, the essential observation for this and all later time points is that the drug fluorescence is predominantly found in the nuclei of the cells, regardless of formulation. The nuclei in the hematoxylin and eosin stained section co-localize precisely with the corresponding location in the fluorescent image. What makes this noteworthy with respect to CAELYX is that it suggests drug leaves the liposome and transits to the nuclear compartment within a very short time. Rarely, we have observed punctate cytoplasmic fluorescence in CAELYX-treated tumours. Abundant punctate cytoplasmic fluorescence might be expected if there were appreciable liposome endocytosis.

2.4. Where does the drug payload separate from the liposome?

Our original strategy was to use a CAELYX formulation double-labeled with both drug and a fluorescent lipid phase marker.. However, it was not possible to establish unequivocally that there was not cross-optical channel interference because doxorubicin has an exceptionally wide absorption spectrum. We compromised by observing CAELYX fluorescence in one tumour and made placebo pegylated STEALTH liposomes containing the fluorescent green phospholipid NBD-DPPE (Molecular Probes, Junction City, OR) to report the disposition of the lipid bilayer.

Fig. 13A, B are cryostat sections from liver which illustrate several points also observed in spleen and tumour 2 h after injection of fluorescent placebo liposomes (Fig. 13A) or CAELYX (Fig. 13B). The nuclei are labeled intensely with drug (A), but there is no labeling of the nuclei with phospholipid (B). The distribution is remarkable for being virtually the 'negative' of the other. The phospholipid distribution labels the plasma membrane and cytoplasmic structures diffusely but not the nuclear membrane or nucleus. There are numerous punctate elements which appear to be both internal and extracellular. Some punctate extranuclear fluorescence is visible in drug-labeled cells (A), as well as the lipid (B). The liver is a very endocytically active organ tissue and circumstantial evidence of internalization is observed. Thus, we do have some reassurance that the experimental conditions and manipulations are capable of observing endocytic uptake. In tumour sections, extranuclear punctate drug fluorescence was a rare occurrence. Since we do see extranuclear fluorescence in the liver and spleen, but not in the tumour, the simplest hypothesis is that the drug becomes 'uncoupled' from the liposomes at an extracellular location in tumours of epithelial origin.

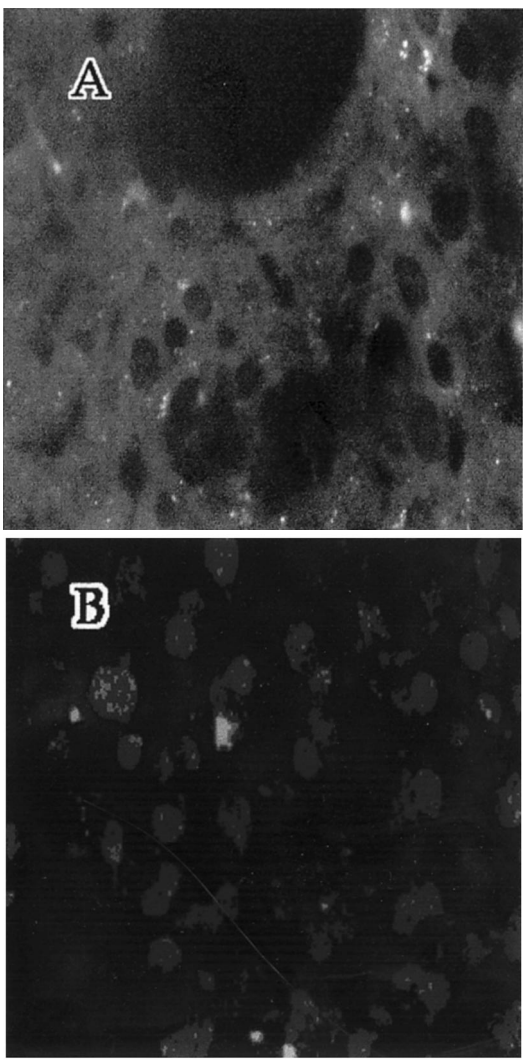

Fig. 13. Fluorescence distribution of phospholipid (A) and the drug (B) in liver, 6 h after injection of equal lipid doses of 6 mg/kg.CAELYX.

3. Conclusions

The extended blood circulation time was one of the first observed phenomena of pegylated STEALTH liposomes (Papahadjopoulos et al., 1991). The consequence of this slow clearance is to provide a prolonged delivery of appreciable quantities of fully-loaded liposomes through tumour vasculature during the first three–four half-lives (about 1.5–2 days in mice). Elsewhere it has been well established that STEALTH liposomes extravasate into the stroma of these regions of increased vascular permeability. For instance, Wu et al. found that pegylated liposomes were taken up by tumours in a far greater quantity than rapidly cleared liposome formulations (Wu et al., 1993). Huang et al. administered colloidal gold-containing STEALTH liposomes to mice transfected with the HIV-tat gene and observed uptake in the lesions' leaky endothelium, but not in adjacent normal skin (Huang et al., 1993).

It was learned from the fluorescence micrograph sequences in these pages that the spatial and temporal pattern of drug concentration is similar from one tumour model to the next. With respect to the absorption phase. Doxorubicin hydrochloride distributes throughout the stroma and the tumour and peaks immediately. In contrast, with CAELYX the initial distribution focalizes in perivascular cells. The drug then permeates through the stroma into the tumour proper during the first 24–48 h.

The time course of drug elimination differs between the drug formulations, but the rate is very similar within the three models. Doxorubicin hydrochloride starts to decline immediately and drops to background levels after 24 h. The drug seems to be 'washed out' evenly throughout the tumour, although the final remnants seem to be adjacent to vascular structures in the wide field view. CAELYX, on the other hand, increases to peak intra-tumour concentrations over 24–48 h and persists for at least 7 days. The persistence appears to be of the nature of a receding wave, as there is still strong labeling persisting near perivascular tissue after a few days.

The majority of intracellular drug fluorescence after CAELYX administration is located inside the nucleus. Despite the negligible drug leakage in plasma (Gabizon et al., 1993), the intra-nuclear drug is observable within minutes after CAELYX administration. However, liposome bilayer labels localize everywhere but inside the nucleus.. This extranuclear location is consistent with the observations of Huang and co-workers, who observed the distribution of colloidal gold-containing STEALTH liposomes in an implanted colon carcinoma to be between perivascular cells, but not intracellularly (Huang et al., 1992.). Given the disjunct intracellular distribution of the drug and the vehicle phospholipid, it would appear that the drug has left the liposomes and is now bioavailable in a compartment with a known mechanism of cytotoxic action. The intratumour AUCs are a measure of nuclear exposure to the drug.

Thus, the sustained delivery of liposomes from the blood compartment, the perivascular deposition of pegylated liposomes, drug leakage and the rapid diffusion of the released drug can account for the temporal and spatial distribution and the markedly increased nuclear drug exposure that we observe after CAELYX administration. The sustained drug exposure of tumour and stromal cells is probably responsible for the enhanced therapeutic effect observed with CAELYX.

Acknowledgements

This research was sponsored by SEQUUS Pharmaceuticals, Inc.

References

Allen, T.M., Chonn, A., 1987. Large unilamellar liposomes with low uptake into the reticuloendothelial system. FEBS Lett. 233 (1), 42–46.

Allen, T.M., Hansen, C., Martin, F., Redemann, C., Yau-Young, A., 1991. Liposomes containing synthetic lipid derivatives of poly(ethylene glycol) show prolonged circulation half-lives in vivo. Biochim. Biophys. Acta 1066, 29–36.

Allen, T.M., Newman, M.S., Woodle, M.C., Mayhew, E., Uster, P.S., 1995. Pharmacokinetics and anti-tumor activity of vincristine encapsulated in sterically stabilized liposomes. Int. J. Cancer 62, 199–204.

Blume, G., Cevc, G., 1990. Liposomes for sustained drug release in vivo. Biochim. Biophys. Acta 1029, 91–97.

Forrsen, E.A., Malé-Brune, R., Adler-Moore, J.P., Lee, M.J.A., Schmidt, P.G., Krasleva, T.B., Shimizu, S., Tromberg, B.J., 1996. Fluorescence imaging studies for the disposition of Daunorubicin liposomes (DaunoXome) within tumor tissue. Cancer Res. 56, 2066–2075.

Gabizon, A., Barenholz, Y., Bialer, M., 1993. Prolongation of the circulation time of doxorubicin encapsulated in liposomes containing a poly(ethylene glycol)-derivatized phospholipid: Pharmacokinetic studies in rodents and dogs. Pharm. Res. 10, 703–708.

Gabizon, A., Shiota, R., Papahadjopoulos, D., 1989. Pharmacokinetics and tissue distribution of doxorubicin encapsulated in stable liposomes with long circulation times. J. Nat. Cancer Inst. 81 (19), 1484–1488.

Gabizon, A.A., 1992. Selective tumor localization and improved therapeutic index of anthracyclines encapsulated in long-circulating liposomes. Cancer Res. 52, 891–896.

Harrison, M., Tomlinson, D., Stewart, S., 1995. Liposomal-entrapped doxorubicin: An active agent in AIDS-related Kaposi's sarcoma. J. Clin. Oncol. 13, 914–920.

Huang, S.K., Lee, K.-D., Hong, K., Friend, D.S., Papahadjopoulos, D., 1992. Microscopic localization of sterically stabilized liposomes in colon carcinoma-bearing mice. Cancer Res. 52, 5135–5143.

Huang, S.K., Martin, F.J., Jay, G., Vogel, J., Papahadjopoulos, D., Friend, D.S., 1993. Extravasation and transcytosis of liposomes in Kaposi's Sarcoma-like dermal lesions of transgenic mice bearing the HIV Tat gene. Am. J. Pathol. 143 (1), 10–14.

Kawai, H., Miniamiya, Y., Kitamura, M., Matsuzaki, I., Hashimoto, M., Suzuki, H., Abo, S., 1997. Direct measurement of doxorubivcin concentration in the intact, living single cancer cell during hyperthermia. Cancer 79, 214–219.

Klibanov, A.L., Maruyama, K., Torchilin, V.P., Huang, L., 1990. Amphipathic polyethleneglycols effectively prolong the circulation time of liposomes. FEBS Lett. 268, 235–237.

Muggia, F.M., Hainsworth, J.D., Jeffers, S., Miller, P., Groshen, S., Tan, M., Roman, L., Uzielly, B., Muderspach, L., Garcia, A., Burnett, A., et al., 1997. Phase II study of liposomal doxorubicin in refractory ovarian cancer: antitumor activity and toxicity modification by liposomal encapsulation. J. Clin. Oncol. 15 (3), 987–993.

Papahadjopoulos, D., Allen, T.M., Gabizon, A., Mayhew, E., Matthay, K., Huang, S.K., Lee, K.-D., Woodle, M.C., Lasic, D.D., Redemann, C., Martin, F.J., 1991. Sterically stabilized liposomes: Improvements in pharmacokinetics and antitumor therapeutic efficacy. Proc. Natl. Acad. Sci. USA 88, 11460–11464.

Senior, J.H., 1988. Fate and behavior of liposomes in vivo: a review of controlling factors. CRC Crit. Rev. Ther. Drug Carrier Systems 3, 123–193.

Siegal, T., Horowitz, A., Gabizon, A., 1995. Doxorubicin encapsulated in sterically stabilized liposomes for the treatment of a brain tumor model: biodistribution and therapeutic efficacy. J. Neurosurg. 83, 1029–1037.

Unezaki, S., Maruyama, K., Hosoda, J.L., Nagae, I., Koyanagai, Y., Nakata, M., Ishida, O., Iwatsura, M., Tsuchiya, S., 1996. Direct measurement of the extravasation of polyethyleneglycol-coated liposomes into solid tumor tissue by in vivo fluorescence microscopy. Int. J. Pharm. 144 (1), 11–17.

Uziely, B., Jeffers, S., Isacson, R., Kutch, K., Wei-Tsao, D., Jehosua, Z., Libson, E., Muggia, F., Gabizon, A., 1995. Liposomal doxorubicin: Antitumor activity and unique toxicities during two complementary phase I studies. J. Clin. Oncol. 13, 1777–1785.

Vaage, J., Donovan, D., Mayhew, E., Abra, R., Huang, A., 1993a. Therapy of human ovarian carcinoma xenografts using doxorubicin encapsulated in sterically stabilized liposomes. Cancer 72 (12), 3671–3675.

Vaage, J., Donovan, D., Mayhew, E., Uster, P., Woodle, M., 1993b. Therapy of mouse mammary carcinomas with vincristine and doxorubicin encapsulated in sterically stabilized liposomes. Int. J. Cancer 54, 959–964.

Vaage, J., Barbera-Guillem, E., Abra, R., Huang, A., Working, P., 1994. Tissue distribution and therapeutic effect of intravenous free or encapsulated liposomal doxorubicin on human prostate carcinoma xenografts. Cancer 73 (5), 1478–1484.

Vaage, J., Donovan, D., Loftus, T., Uster, P., Working, P., 1995. Prophylaxis and therapy of mouse mammary carcinomas with doxorubicin and vincristine encapsulated in sterically stabilized liposomes. Eur. J. Cancer 3 (1995), 367–372.

Vaage, J., Donovan, D., Uster, P., Working, P., 1997. Tumor uptake of doxorubicin in polyethylene-glycol coated liposomes and therapeutic effect against a xenografted human pancreatic carcinoma. Br. J. Cancer 75 (4), 482–483.

Vail, D.M., Kravis, L.D., Cooley, A.J., Chun, R., MacEwan, E.G., 1997. Preclinical trial of doxorubicin entrapped in sterically stabilized liposomes in dogs with spontaneously arising malignant tumors. Cancer Chemother. Pharmacol. 39, 410–416.

Wu, N.Z., Da, D., Rudoll, T.L., Needham, D., Whorton, R., Dewhirst, M.W., 1993. Increased microvascular permeability contributes to preferential accumulation of STEALTH liposomes in tumor tissue. Cancer Res. 53, 3765–3770.

Zhu, G., Oto, E., Vaage, J., Quinn, Y., Newman, M., Engbers, C., Uster, P., 1996. The effect of vincristine-polyanion compleses in STEALTH liposomes on pharmacokinetics, toxicity and anti tumor activity. Cancer Chemother. Pharmacol. 39, 138–142.

.